BMBAD BJESR Mühendislik Bilimleri ve Araştırmaları Dergisi
Journal of Engineering Sciences and Researches

Coil Design and Optimization for Wireless Charging Applications of Electric Vehicles

Elektrikli Araçların Kablosuz Şarj Uygulamaları için Bobin Tasarımı ve Optimizasyonu

[1]Cem KUTLU, [2]Harun ÖZBAY

[1,2]Bandırma Onyedi Eylül Üniversitesi, Mühendislik ve Doğa Bilimleri Fakültesi, Bandırma/Balıkesir, Türkiye

[1]cem.kutlu@ogr.bandirma.edu.tr, [2]hozbay@bandirma.edu.tr

Araştırma Makalesi/Research Article

ARTICLE INFO

Article history

Received : 1 October 2025
Accepted : 16 November 2025

Keywords:

Inductive Power Transfer, Coil Design, Electric Vehicles, Wireless Charging

ABSTRACT

The growing adoption of electric vehicles has led to an increased demand for high-efficient wireless power transfer (WPT) systems, wherein coil design plays a pivotal role in determining performance. The present study proposes an integrated design and optimization methodology that addresses the electromagnetic and circuit-level analyses through co-simulation in Ansys Maxwell and Simplorer. The findings demonstrate the consistent attainment of the 7.7 kW power objective, with an output of 7.8 kW and a transfer efficiency of 98% achieved through the optimization of the coil turn number under the Maximum Power Transfer (MPT) condition. The outcomes furnish a systematic framework for balancing efficiency and power output, thereby confirming the coil design's viability for practical electric vehicle charging applications.

MAKALE BİLGİSİ

Makale Tarihleri

Gönderim : 1 Ekim 2025
Kabul : 16 Kasım 2025

Anahtar Kelimeler:

Endüktif Güç Transferi, Bobin Tasarımı, Elektrikli Araçlar, Kablosuz Şarj

ÖZET

Elektrikli araçların giderek daha fazla benimsenmesi, yüksek verimli kablosuz güç aktarım (WPT) sistemlerine olan talebin artmasına neden olmuştur. Bu sistemlerde, bobin tasarımı performansın belirlenmesinde çok önemli bir rol oynamaktadır. Bu çalışmada, Ansys Maxwell ve Simplorer'da ortak simülasyon yoluyla elektromanyetik ve devre düzeyindeki analizleri ele alan entegre bir tasarım ve optimizasyon metodolojisi önerilmektedir. Bulgular, Maksimum Güç Aktarımı (MPT) koşulu altında bobin tur sayısının optimizasyonu ile 7.8 kW çıkış gücü ve %98 aktarım verimliliği elde edilerek 7.7 kW güç hedefinin tutarlı bir şekilde gerçekleştirildiğini göstermektedir. Sonuçlar, verimlilik ve güç çıkışı arasında denge sağlamak için sistematik bir çerçeve sunarak, bobin tasarımının elektrikli araç şarj uygulamaları için uygunluğunu teyit etmektedir.

ORCID ID: [1]0000-0003-4457-7197
[2]0000-0003-1068-244X

1. INTRODUCTION

The accelerated adoption of electric mobility has given rise to novel challenges and opportunities, particularly in the development of efficient and user-friendly charging infrastructure. Despite their extensive implementation, conventional plug-in charging systems exhibit numerous limitations. These include connector wear, electrical safety concerns, weather dependence, and user inconvenience [1],[2]. WPT technology has emerged as a promising solution to these challenges, offering seamless charging experiences by allowing electric vehicles to charge simply by parking over a charging pad without any physical connections [3],[4]. The integration of this technology into the charging infrastructure not only enhances convenience for end users but also addresses critical safety concerns associated with exposed electrical connections. Moreover, it enables the transition to autonomous charging capabilities, a significant advancement in the field of energy storage and management [5].

The WPT system operates based on the same fundamental mechanism as an ordinary transformer. However, it uses transmitting and receiving coils with low coupling, apart by an air gap [6]. This leads to a high leakage flux of noncoupled coils compared to conventional transformers, and the efficiency can be significantly reduced [7]. Magnetic resonance coupling represents the optimal approach for wireless charging of electric vehicles. This method facilitates efficient energy transfer through electromagnetic induction between magnetically coupled coils [8]. The WPT system is composed of primary (transmitter) and secondary (receiver) coils that establish a magnetic coupling for power transfer [9]. However, the performance of these systems is contingent upon the design parameters of the inductive coils, including geometry, material selection, and coupling configuration. The coupling coefficient and load resistance in WPT systems are frequently uncertain and variable in numerous applications, affecting both output power and system efficiency significantly, particularly during dynamic applications. For instance, if the coupling coefficient decreases due to coil misalignment or if the actual load resistance no longer matches the optimum value, the efficiency can be significantly reduced [10].

Despite the simplicity and ease of use offered by inductive power transfer (IPT) systems, they face significant technical challenges including leakage inductance, power losses, and efficiency degradation [11]. Research has shown that factors such as air gap distance and coil misalignment critically affect the coupling coefficient, coil inductance, and mutual inductance, directly impacting the overall system efficiency [12]. These challenges necessitate precise optimization of coil design parameters to achieve acceptable power transfer efficiency.

Recent studies have focused on various aspects of WPT coil optimization, including advanced compensation topologies [13], bidirectional power transfer capabilities [14], and intelligent control systems [15]. Advanced optimization techniques such as neural networks and bio-inspired algorithms have been employed to enhance coil design and control strategies for improved WPT performance [16]. However, there remains a need for comprehensive analysis combining electromagnetic field simulation with circuit-level performance evaluation to fully understand the relationship between coil design parameters and system efficiency.

This study presents a systematic approach to coil design and analysis for wireless electric vehicle charging applications. The research employs the electromagnetic field analysis and the circuit simulation to provide a comprehensive evaluation of coil performance. The primary objectives include optimizing coil geometry for maximum power transfer efficiency and validating the design through integrated electromagnetic-circuit simulations. The findings of this work contribute to the development of more efficient and practical wireless charging solutions for the rapidly expanding electric vehicle market.

2. IPT SYSTEM

IPT system is composed of two coils positioned in opposition, with an air gap separating them. In WPT scenarios, a magnetic field is created within the transmitter coil. This field is picked up by the receiver coil resulting a voltage. The primary components of an IPT system, the most prevalent among WPT methods, consist of a direct current (DC) power supply, an inverter, primary and secondary compensation units, a magnetic coupling unit, a rectifier, and a load. The DC voltage is converted to high-frequency AC voltage by the inverter. The primary compensation unit has been shown to optimize the transmitter power, thereby improving energy transfer efficiency. The optimized voltage is known to generate a magnetic field within the transmission coil. The transmission coil is responsible for the conversion of magnetic field energy into electrical energy, thereby powering the load. This process is known as magnetically coupled wireless power transmission [17].

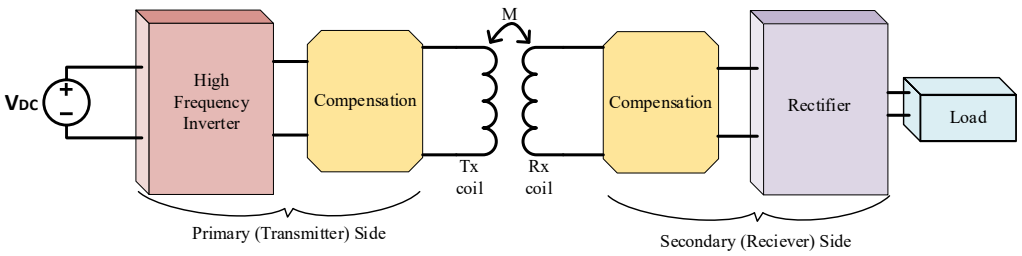

Figure 1. IPT system block diagram.

The IPT block diagram is illustrated in Figure 1. This structure includes additional compensation networks as compared to a traditional IPT system. These compensation topologies are incorporated into both the transmitter and receiver sides with the objective of creating resonance and reducing additional losses. The matching of the resonant frequencies of the primary and secondary windings is a prerequisite for efficient power transfer.
The integration of transceiver coils is paramount to achieving efficacious results [18]. The relationship between mutual inductance M and the coupling coefficient k is expressed by equation 1.

$$M = k\sqrt{L_1 L_2} \tag{1}$$

2.1. Compensation Topologies

The presence of inductive properties in the coils results in the consumption of reactive power within the IPT system. Reactive power consumption exhibits a marked decrease in efficiency, particularly in high-frequency applications. Therefore, in order to facilitate the efficient transfer of power without the concomitant consumption of reactive power, it is imperative that the inverter operate at a phase angle of zero. This condition necessitates that the output voltage and current be in phase. The attainment of this objective is dependent upon the system operating at its resonant frequency[19].

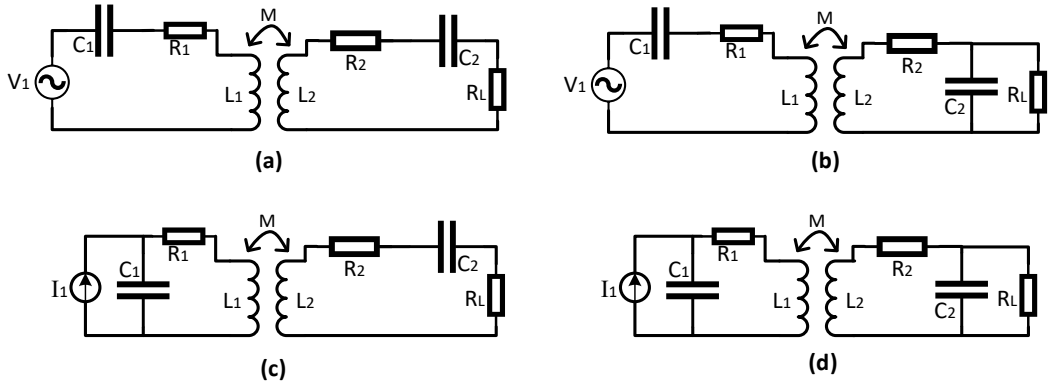

Figure 2. Conventional compensation topologies a) SS, b) SP, c) PS and d) PP.

Within the framework of IPT systems, the integration of compensation mechanisms into both the primary (transmitter) and secondary (receiver) coil assemblies is instrumental in ensuring the efficacy of the overall system. This integrated approach enables the optimization of power transfer, thereby ensuring efficient operation. These systems ensure high quality factors, thereby facilitating more efficient and reliable power transfer. In IPT systems utilized in electric vehicles (EVs), compensation is typically executed at the resonant frequency.
Resonant circuits optimize transmission efficiency by maximizing the transferred power [20]. This enhancement is achieved by means of two mechanisms: the primary mechanism involves the balancing of the magnetizing current in the transmitter coil, while the secondary mechanism involves the suppression of higher harmonics [21].
The configuration of conventional compensation topologies, encompassing the series-serial (SS), series-parallel (SP), parallel-series (PS), and parallel-parallel (PP) circuits, is delineated in Figure 2(a), (b), (c), and (d), respectively.
A number of advantages are offered by these compensation networks, including soft switching, constant voltage-current, misalignment tolerance, power ripple reduction, and power transfer capabilities. The SS-type compensation network is among the most prevalent topologies and exhibits a constant output current characteristic. The capacitance value of the SS-type compensation network is independent of the mutual inductance and load. Therefore, the WPT system maintains resonance even in the presence of coil balance or load fluctuations [17].
The performance of basic compensation topologies is optimized under ideal conditions. However, factors such as misalignment and frequency drift have the potential to compromise the efficiency of wireless charging systems. The literature has frequently proposed hybrid configurations that integrate the benefits of diverse topologies.
Each hybrid structure exhibits a unique set of advantages and disadvantages. Hybrid topologies offer various advantages, including enhanced system efficiency against misalignment, reduced electromagnetic interference, simultaneous charging of multiple devices, and the establishment of bidirectional charging systems [21].

2.2. IPT System Analysis

The circuit configuration of an IPT system designed for a wireless charging solution in electric vehicles is presented in Figure 3. An inverter, positioned on the ground side of the charger, generates an alternating voltage of high frequency. This voltage is subsequently applied to the transmitter coil. The square wave is capable of producing a time-varying magnetic field. The induction of voltage in the vehicle-side coil is a result of the mutual coupling between the two coils, as governed by the magnetic field. The induced voltage undergoes rectification and is then utilized to power the load, which in this case is a battery pack [22].
The electrical analysis of the WPT system is facilitated by the derivation of a suitable equivalent circuit model depicted in Figure 4.

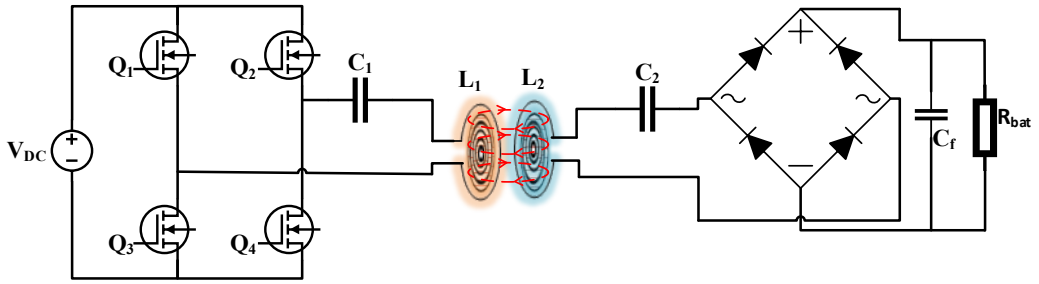

Figure 3. Circuit model of the WPT system.

The rectifier, filter capacitor (C_f) and battery (R_{bat}) can be replaced with the equivalent AC resistance (R_L) which is seen from the primary side is calculated using equation 3. In this model, L, R, C, Z and M represents inductance, resistance, capacitance, impedance and mutual inductance respectively. In the context of the given equations 4-5-6, subscript 1 is designated as the primary side, whereas subscript 2 is denoted as the secondary side [23].

$$R_{bat} = \frac{{V_{bat}}^2}{P_{bat}} \tag{2}$$

$$R_L = \frac{8}{\pi^2} \cdot R_{bat} \tag{3}$$

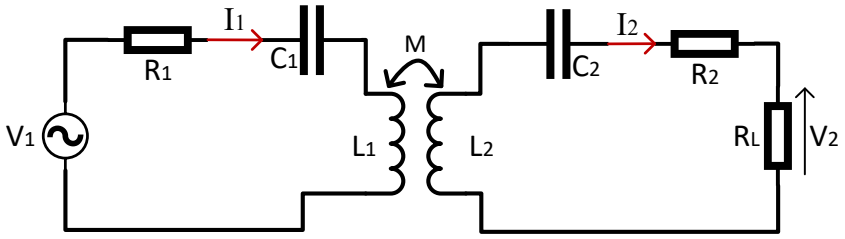

Figure 4. Equivalent model of the series-series compensated WPT system.

According to the equivalent circuit model for the series-series topology, there is the following definition for the model.

$$\begin{bmatrix} V_1 \\ 0 \end{bmatrix} = \begin{bmatrix} Z_1 & j\omega M \\ j\omega M & Z_2 \end{bmatrix} \begin{bmatrix} I_1 \\ I_2 \end{bmatrix} \tag{4}$$

$$Z_1 = R_1 + j\omega L_1 + \frac{1}{j\omega C_1} \tag{5}$$

$$Z_2 = R_2 + R_L + j\omega L_2 + \frac{1}{j\omega C_2} \tag{6}$$

Therefore, it can be concluded that the transmitter and receiver side currents of the equivalent circuit can be expressed in the following equations 7-8.

$$I_1 = \frac{V_1 \cdot Z_2}{(\omega M)^2 + Z_1 \cdot Z_2} \tag{7}$$

$$I_2 = \frac{j\omega M V_2}{(\omega M)^2 + Z_1 \cdot Z_2} \tag{8}$$

The voltages induced in the receiver and transmitter coils, designated as $V_{2,ind}$ and $V_{1,ind}$, respectively, are defined in terms of the mutual inductance between the two coils, as delineated in equations 9-10.

$$V_{2,ind} = j\omega M I_1 \tag{9}$$

$$V_{1,ind} = -j\omega M I_2 \tag{10}$$

The reflected impedance, denoted by Z_r, can be delineated by equation 11.

$$Z_r = \frac{-j\omega M I_2}{I_1} = \frac{\omega^2 M^2}{Z_2} \tag{11}$$

Therefore, the impedance that can be seen from the transmitter is given by equation 12.

$$Z_{in} = Z_1 + Z_r\,, \qquad Z_{in} = Z_1 + \frac{\omega^2 M^2}{Z_2} \tag{12}$$

At the resonant frequency, I_1 and power transfer efficiency η can be expressed by equations 13-14 respectively.

$$I_1 = \frac{V_1(R_2 + R_L)}{(\omega M)^2 + R_1(R_2 + R_L)} \quad (13)$$

$$\eta = \frac{P_{out}}{P_{in}} = \frac{R_L I_2^2}{V_1 I_1} = \frac{R_L\,(\omega M)^2}{(R_2 + R_L)\,(R_1\,(R_L + R_2) + (\omega M)^2)} \quad (14)$$

3. COIL DESİGN

In WPT systems, coil design constitutes a pivotal step in achieving high efficiency. In the domain of WPT, circular and rectangular planar coils have emerged as predominant coil architectures employed in WPT chargers. As illustrated in Figure 5, circular coil pair models are presented for guidance.

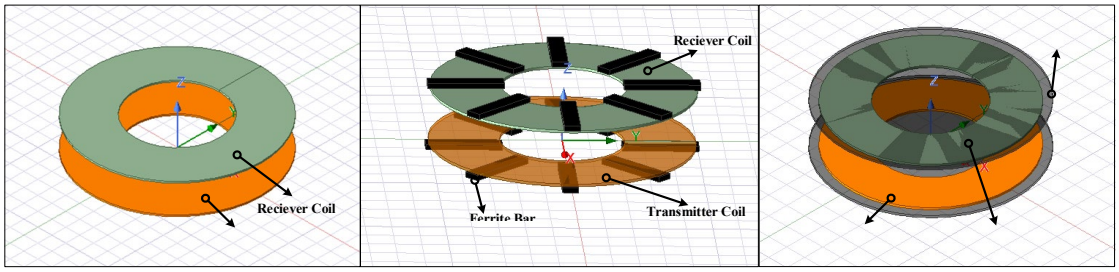

Figure 5. Examples of the circular transceiver coils a)coreless coil pair b)coil pair with ferrite bar c)coil pair with ferrite plate.

Despite the fact that ferrite plate configuration offers superior electromagnetic performance as given in Table 1, the ferrite bar core design shown in Figure 5b was selected for this study due to practical implementation considerations. The ferrite bar offers an acceptable trade-off between performance and practicality, providing a significant reduction in weight and material cost compared to the ferrite plate while still improving efficiency over the coreless design. Furthermore, the bar configuration facilitates seamless integration into vehicle underbody structures, rendering it particularly well-suited for real-world electric vehicle applications where weight, cost, and packaging constraints are paramount.

Table 1. The effect of ferrite on coupling at transceiver coils for $N = 17, Z_{dist} = 150mm, D_{out} = 500mm$

	Coreless	With Ferrite Bar	With Ferrite Plate
k	0.229	0.268	0.332
M	$28.56\mu H$	$45.37\mu H$	$76.62\mu H$
$L_{1,2}$	$124.71\mu H$	$169.29\mu H$	$230.78\mu H$

3.1. Design Parameters

The utilization of finite element analysis (FEA) by Ansys software constitutes a highly effective solution for problems pertaining to electromagnetic fields. FEA is a method that facilitates precise calculation of crucial variables such as magnetic flux density, inductance, losses etc. and it involves the subdivision of the region to be investigated into a finite number of smaller elements, thereby creating a mesh. Each small region or element is analyzed in detail to provide an approximate solution for the problem [24].

The present study implements the coil design of a IPT system for 7.7 kW power transmission. The preliminary stage entails the specification of the initial parameters, followed by the calculation of the electrical parameters. The operating frequency of 85 kHz is selected in accordance with the SAE J2954 standard, a set of specifications established by the Society of Automotive Engineers (SAE) for the design, construction, and testing of wireless charging systems intended for lightweight plug-in electric vehicles [25]. Accordingly, the angular frequency, designated as ω_r is determined through the application of equation 15.

$$\omega_r = 2\pi f_r \quad (15)$$

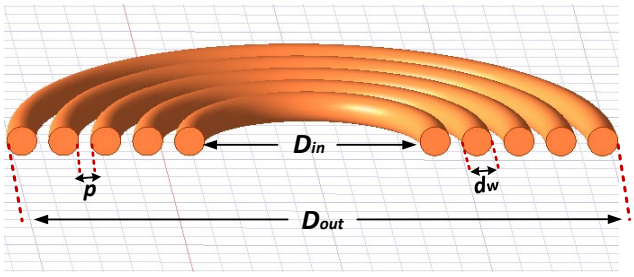

Figure 6. Section of the YZ plane view of a circular coil.

As illustrated in Figure 6, the model under consideration consists of a circular coil shown in its section of YZ plane. Equation 16 provides a calculation of the D_{out} value, wherein the D, p and d_w parameters denote the coil diameter, the space between each turn and the wire diameter, respectively.

$$D_{out} = D_{in} + 2d_w N + 2p(N-1) \tag{16}$$

The total length of the copper wire in meters l_{cu} is given by equation 17.

$$l_{cu} = \frac{\pi . N\ (D_{in} + D_{out})}{200} \tag{17}$$

Therefore, the resistance can be expressed as follows:

$$R = \frac{\rho\ l_{cu}}{S_c} \tag{18}$$

$\rho = 1.68 \times 10^{-8} \Omega m$ represent the resistivity of copper. The cross-sectional area of copper S_c is given by equation 19.

$$S_c = \frac{\pi}{4} \cdot d_w^2 \tag{19}$$

3.2. Electrical Characteristics

The subsequent step involves the determination of the electrical parameters. The capacitor values necessary for the series resonance circuit can be ascertained through the application of equation 20 and the quality factor can be expressed by equation 21.

$$C_1 = \frac{1}{\omega^2 L_1}, \qquad C_2 = \frac{1}{\omega^2 L_2} \tag{20}$$

$$Q_2 = \frac{\omega_0 L_2}{R_L} \tag{21}$$

In a similar manner, in order to extract the maximum transmission efficiency, the load must be maximized. This can be achieved by finding the optimal load for the given transmission conditions. To derive the efficiency expression as a function of load, refer to equation 22.

$$\frac{d\eta}{dR_L} = \frac{d\left(\frac{R_L\ (\omega M)^2}{(R_2 + R_L)\ (R_1\ (R_L + R_2) + (\omega M)^2)}\right)}{dR_L} = 0$$

$$(R_2 + R_L)[R_1(R_L + R_2) + (\omega M)^2] - R_L[2R_1(R_L + R_2) + (\omega M)^2] = 0 \tag{22}$$

$$R_L = R_2\sqrt{1 + \frac{(\omega M)^2}{R_1 R_2}}$$

The transmitted power of a WPT system is denoted by P_{tx} [26].

$$P_{tx} = \frac{\omega_0\ {I_1}^2\ M^2\ Q_2}{L_2} = \frac{{\omega_0}^2 {I_1}^2 M^2}{R_L} \tag{23}$$

3.3. Coil Design Application for IPT System

The present section is focused on the implementation of the methodology for designing a series-series WPT system. The objective of the analysis is to ascertain the coil parameters necessary to facilitate the transfer of 7.7 kW of power to the vehicle's battery. The preliminary design parameters are delineated by the power to be transferred, P_{tx}, the battery voltage, V_{bat}, the conductor diameter, d_w , the distance between coils, Z_{dist} , and the outer diameter of the primary coil, D_{out}. Their respective values are provided in Table 2.

Assuming that the winding will be done with a gap between the conductors of p=1mm, the coil model was simulated for N=16 using the initial parameters and the inner diameter value calculated in equation 24.

$$400mm = D_{in} + (2\ x\ 5mm\ x\ 16) + (2\ x1mm\ x15) \tag{24}$$

Table 2. Initial parameters for WPT system design.

Parameter	Value
D_{out}	400mm
d_w	5mm
V_{bat}	400V
Z_{dist}	100mm
P_{tx}	7.7kW

For $N = 16$, the L_1, L_2 and M values obtained from the simulation results are presented in Table 3. To determine the power transferred, the source current I_1 must be calculated.
The coil design is to be tested to ensure that it delivers the desired power and will be optimized until the desired power transfer is achieved, for which the flowchart shown in Figure 7 and equations from the previous section are to be applied. In instances where the input voltage and the nominal battery voltage are both set at 400V, and the target power P_{tar} is established at 7.7kW, the resistance of the battery model can be calculated by using equation 25.

$$R_{bat} = \frac{{V_{bat}}^2}{P_{bat}} = 20.77\Omega \tag{25}$$

The total equivalent load resistance is computed utilizing equation 26.

$$R_L = \frac{8}{\pi^2} \cdot R_{bat} = 16.83\Omega \tag{26}$$

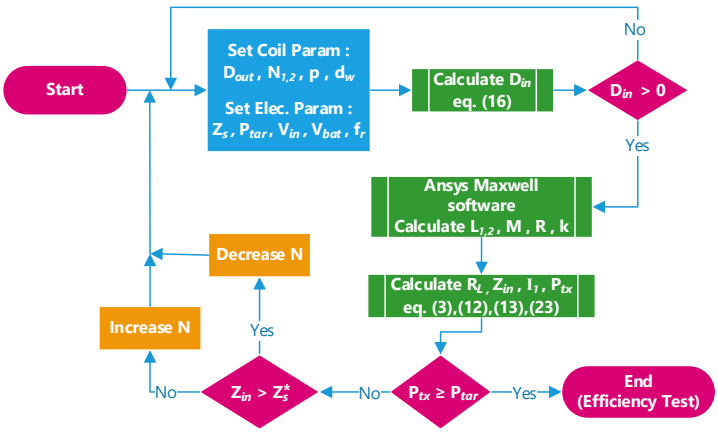

Figure 7. Flowchart of the coil design optimization.

At the resonant frequency of the system, if the resistors R_1 and R_2 are negligible in equation 13, then the current I_1 can be readily calculated using equation 27.

$$I_1 = \frac{V_1 R_L}{(\omega M)^2} = 12.58A \tag{27}$$

Subsequently, determining the current of the primary side enables the calculation of the power value that can be transferred, as given by equation 28.

$$P_{tx} = \frac{{\omega_0}^2 {I_1}^2 M^2}{R_L} = 5035W \tag{28}$$

The power calculation indicates that the present parameters result in a power output that falls short of the desired target. It is possible to experiment with different coil parameters to increase the transferred power; however, in this study, the number of turns N and therefore the coil's internal diameter D_{in} were changed, while the coil outer diameter D_{out} remained constant at 400mm, the conductor diameter d_w at 5mm, distance Z_{dist} between Tx-Rx coils at 100mm and the turn spacing p at 1mm, to achieve a power transfer of 7.7kW.
I_1 and M display an opposing behavior, a concept clearly shown within equation 13. A reduction in the value of M results in a decrease in the impedance reflected (Z_r) from the receiver side and an increase in the current drawn from the source. Consequently, the amount of power supplied by the source will concomitantly increase. This indicates that decreasing the value of M necessitates a reduction in the conductor length, the number of turns N. This process is repeated iteratively, with each subsequent iteration involving a change in the number of turns and an estimation of the inner diameter using equation 16. Following this, the self-inductance and mutual inductance values are determined for the specified coil design. The transferred power is thereafter calculated using equation 23, and the process is deemed complete if the calculated value is equal or greater than the target power which is 7.7 kW in this study.

Table 3. Iteration results of different N values for $Z_{dist} = 100mm$.

	N=16	N=15	N=14
k	0.32	0.31	0.30
M	$43.30\mu H$	$38.63\mu H$	$34.88\mu H$
$L_{1,2}$	$133.86\mu H$	$122.40\mu H$	$116.27\mu H$
P_{tx}	$5.03kW$	$6.32kW$	$7.75kW$

The objective of the simulation was to identify the most suitable design capable of effectively transferring the desired

power. In order to facilitate analysis, both the transmitter and receiver coils were designed to have equivalent dimensions. As indicated by the results presented in Table 3, the targeted power value was attained in iteration $N = 14$.

3.4. Efficiency Test of the Designed Coil

The performance of the coil designed in the previous section was evaluated by means of a simplified circuit which is the equivalent circuit model of the system. The primary part of the circuit is powered by a square wave voltage source matched to an inverter output voltage, and resonant capacitors are incorporated into the circuit on both sides. The modeling and circuit analysis were performed by co-simulating the Ansys Maxwell and the Ansys Simplorer environment.

Transceiver coils created in accordance with the design methodology outlined in the previous section, was imported into circuit model for the purpose of executing the computational evaluation of the setup. Figure 8 presents the electrical schematic corresponding to the equivalent model.

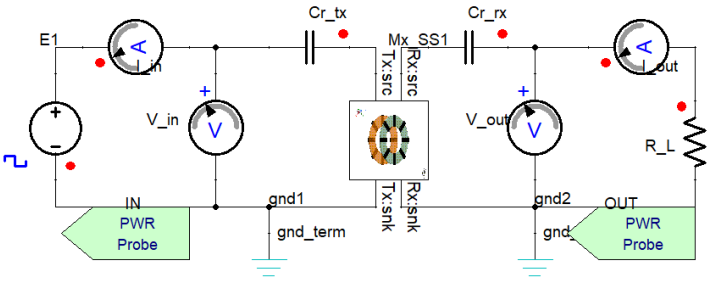

Figure 8. Equivalent circuit of WPT system.

Since the resonance frequency of the circuit and the inductance values determined according to the simulation results are known, the capacitance values C_{r_tx} and C_{r_rx} also can be calculated with equation 29.

$$C_{r\_tx} = C_{r\_rx} = \frac{1}{\omega^2 L_1} = 30.15nF \tag{29}$$

While conventional WPT theory often targets a high mutual inductance M or coupling coefficient k to maximize system efficiency and power transfer, the scenario aiming for a specific $7.7kW$ power draw highlights a shift in design focus toward source-side input impedance matching.

The system's inability to draw the target power (only achieving $5kW$ with $N = 16$ and $k = 0.32$) indicates that the reflected impedance Z_r from the receiver side was excessively high for this configuration, leading to a mismatch with the source impedance.

The controlled reduction of mutual inductance M by decreasing the number of turns to $N = 14$ (and coupling to $k = 0.3$) lowered the reflected impedance, according to the relationship $Z_r \propto \omega^2 M^2$. This decrease in reflected impedance reduced the system's total input impedance Z_{in} and, under a fixed source voltage, increased the current I_1 drawn from the source. This process effectively guided Z_{in} towards the optimal value, which must equal the Z_s^*, complex conjugate of the source impedance to satisfy the condition for Maximum Power Transfer (MPT). This approach ensures $Z_{in} = Z_s^*$ which is necessary to achieve the target power draw of 7.7 kW, therefore successfully satisfying the MPT condition.

This analysis underscores the necessity of optimizing the system's input impedance relative to the source in order to achieve a specific power target, emphasizing that high coupling alone is insufficient for this purpose. The simultaneous realization of high transferred power (7.8 kW) and high efficiency (η=98%) through a controlled reduction in M demonstrates that the optimal design does not depend on the absolute magnitude of M, but rather on its capacity to reflect the load impedance optimally to the source. Therefore, the determination of the N or M value should be informed not only by geometric constraints but primarily by the requirements of matching the input impedance Z_{in} to the source conjugate Z_s^*.

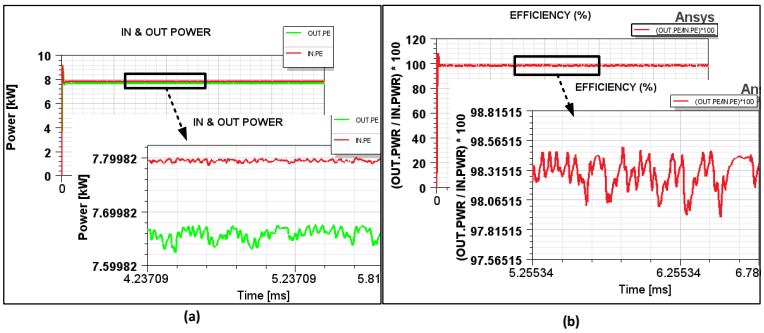

(a) (b)

Figure 9. (a)The transmitted and received power values of equivalent WPT circuit (b)Time-Efficiency graph of designed transceiver coils.

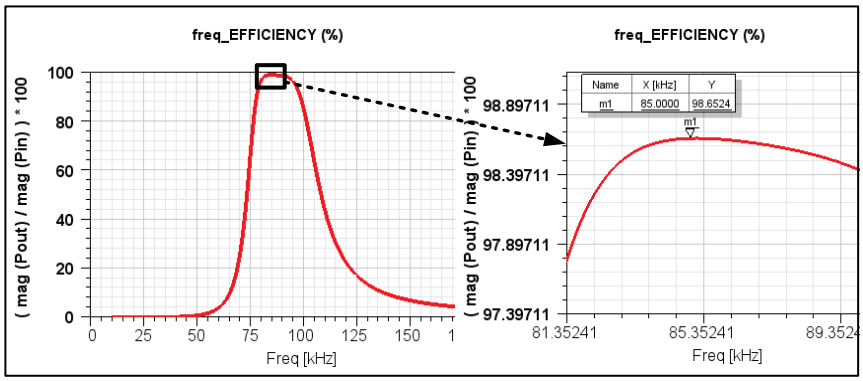

Figure 10. Frequency-Efficiency graph of designed transceiver coils.

4. CONCLUSION

This study presents a comprehensive investigation of WPT coil design for electric vehicle charging applications through an integrated simulation approach combining electromagnetic field analysis and circuit-level performance evaluation. The designed and optimized coils were integrated into an equivalent WPT circuit model so that a thorough performance analysis and validation might be conducted. The results of the simulation demonstrate a high degree of agreement between the theoretical predictions and the computational analysis for the target power transfer of 7.7 kW. As demonstrated in Figure 9a, the input power source delivers approximately 7.8 kW, a value that closely aligns with the design specifications outlined in theory. A critical finding of the analysis that shown in Figure 9b-10 is that over 98% of the input power (approximately 7.6 kW) is successfully transmitted to the receiver side. This was achieved by optimizing the primary-side input impedance through a controlled adjustment of the coil turns, thereby satisfying the Maximum Power Transfer condition necessary to meet the 7.7 kW power target**.**

The simultaneous realization of high-power transfer and a remarkable efficiency confirms the potential for this design to be further optimized and adapted to meet varying power requirements for different electric vehicle charging scenarios. The integration of electromagnetic field simulation with circuit-level analysis has been demonstrated to yield valuable insights into the relationship between coil geometry, electromagnetic behavior, and overall system performance. This integrated approach not only validates the theoretical design principles but also establishes a robust framework for future coil optimization studies.

In the context of future research endeavors, a comparative performance evaluation will be conducted between circular and square coil geometries within a comprehensive system architecture that incorporates inverter and rectifier components. Furthermore, the analysis will be expanded to encompass misalignment scenarios, which represent critical real-world operating conditions in the context of electric vehicle wireless charging applications. This comprehensive evaluation will provide deeper insights into the practical implementation challenges and performance trade-offs associated with different coil configurations under various operational conditions.

Author Contribution

The authors contributed equally to all stages of the study, including its design, execution, data analysis, result evaluation, and paper writing.

Conflict of Interest

The authors of the article declare that they have no conflict of interest.

REFERENCES

[1] M.T. Tran, S. Thekkan, H. Polat, D.D. Tran, M. El Baghdadi and O. Hegazy, “Inductive Wireless Power Transfer Systems for Low-Voltage and High-Current Electric Mobility Applications: Review and Design Example”, MDPI, 2023.

[2] H. Özbay, C. Közkurt, A. Dalcalı and M. Tektaş, “Geleceğin Ulaşım Tercihi: Elektrikli Araçlar”, Akıllı Ulaşım Sistemleri ve Uygulamaları Dergisi, vol. 3, no. 1, pp. 34–50, 2020.

[3] V. Ramakrishnan et al., “Design and Implementation of a High Misalignment-Tolerance Wireless Charger for an Electric Vehicle with Control of the Constant Current/Voltage Charging”, Scientific Reports, vol. 14, no. 1, 2024.

[4] B. Latha, M.M. Irfan, B.K. Reddy and C.H.H. Basha, “A Novel Enhancing Electric Vehicle Charging: An Updated Analysis of Wireless Power Transfer Compensation Topologies”, Springer Nature, 2025.

[5] V. Ramakrishnan, A.D. Savio, M. Shorfuzzaman and W.M. Abdelfattah, “An Enhanced Vehicle-to-Vehicle Wireless Power Transfer System for Electric Vehicle Applications Using a Reconfigurable Coil Approach”, IEEE Access, vol. 13, pp. 9931–9941, 2025.

[6] A. Sagar et al., “A Comprehensive Review of the Recent Development of Wireless Power Transfer Technologies for Electric Vehicle Charging Systems”, IEEE Access, vol. 11, pp. 83703–83751, 2023.

[7] H.T. Nguyen et al., "Review Map of Comparative Designs for Wireless High-Power Transfer Systems in EV Applications: Maximum Efficiency, ZPA, and CC/CV Modes at Fixed Resonance Frequency Independent from Coupling Coefficient", IEEE Transactions on Power Electronics, vol. 37, no. 4, pp. 4857–4876, 2022.

[8] Y. Özüpak, "Analysis and Experimental Verification of Efficiency Parameters Affecting Inductively Coupled Wireless Power Transfer Systems", Heliyon, vol. 10, no. 5, 2024.

[9] V. Sari, "Design and Implementation of a Wireless Power Transfer System for Electric Vehicles", World Electric Vehicle Journal, vol. 15, no. 3, 2024.

[10] J. Cai, X. Wu, P. Sun, J. Sun and Q. Xiong, "Optimization Design of Zero-Voltage-Switching Control in S-LCC Inductive Power Transfer System Under Dynamic Coupling Coefficient", Journal of Electrical Engineering & Technology, vol. 16, no. 6, pp. 2937–2948, 2021.

[11] M.M.R. Ahmed et al., "Optimized Design and Sizing of Wireless Magnetic Coupling Stage for Electric Vehicle-to-Grid (V2G) Charging Station", Scientific Reports, vol. 15, no. 1, 2025.

[12] R.B.Y. Alsuwaidi, A.G. Abokhalil, M. El Haj Assad and A.A. Hassan, "Wireless Charging for Electric Vehicles: The Impact of Air Gap Distance and Coil Alignment on Power Transfer Efficiency", International Youth Conference on Radio Electronics, Electrical and Power Engineering (REEPE), 2025.

[13] M. Venkatesan, N. R, P. Kacor and M. Vrzala, "Bidirectional Wireless Power Transfer: Bridging Electric Vehicles and the Grid Through Converter Analysis, Coil Topologies, and Communication Protocol Review", Elsevier, 2025.

[14] A. Mubarak, A.A. Amin, M. Ahmad, M.F. Shafique and M.S. Zafar, "Wireless Power Transfer for Deep Cycle Lithium-Ion Batteries in Electric Vehicles Using Inductive Coupling", Advances in Mechanical Engineering, vol. 16, no. 10, 2024.

[15] Z. Xue, W. Liu, C. Liu and K.T. Chau, "Critical Review of Wireless Charging Technologies for Electric Vehicles", World Electric Vehicle Journal, vol. 16, no. 2, 2025.

[16] K. Thiagarajan, T. Deepa and M. Kolhe, "Optimized Coil Design and Advanced Neural Network Control for Enhanced Wireless Power Transfer in Electric Vehicles Using Taylor-Based Firefly and Dove Swarm Optimization", Wireless Power Transfer, vol. 11, no. 1, 2024.

[17] K. Li, J. Chen, X. Sun, G. Lei, Y. Cai and L. Chen, "Application of Wireless Energy Transmission Technology in Electric Vehicles", Renewable and Sustainable Energy Reviews, vol. 184, 2023.

[18] T. Bouanou, H. El Fadil, A. Lassioui, O. Assaddiki and S. Njili, "Analysis of Coil Parameters and Comparison of Circular, Rectangular, and Hexagonal Coils Used in WPT System for Electric Vehicle Charging", World Electric Vehicle Journal, vol. 12, no. 1, 2021.

[19] H. Khalid, S. Mekhilef, M. Mubin and M. Seyedmahmoudian, "Advancements in Inductive Power Transfer: Overcoming Challenges and Enhancements for Static and Dynamic Electric Vehicle Applications", Energy Reports, vol. 10, pp. 3427–3452, 2023.

[20] C. Kutlu and H. Özbay, "Design of PV Based ZVS SEPIC Converter for Electric Vehicle Battery Charger", International Symposium of Scientific Research and Innovative Studies, pp. 1084–1092, 2022.

[21] A.H. Reyhan and A. Doğan, "Elektrikli Araçların Kablosuz Şarj Edilmesinde Kullanılan Güç Aktarım Yöntemlerinin İncelenmesi", Ömer Halisdemir Üniversitesi Mühendislik Bilimleri Dergisi, vol. 12, no. 4, pp. 1305–1317, 2023.

[22] I. Bentalhik et al., "Analysis, Design and Realization of a Wireless Power Transfer Charger for Electric Vehicles: Theoretical Approach and Experimental Results", World Electric Vehicle Journal, vol. 13, no. 7, 2022.

[23] H. Özbay, "Rezonans Dönüştürücülü Fotovoltaik Batarya Şarj Sistemi", Bandırma Üniversitesi Mühendislik ve Doğa Bilimleri Dergisi, vol. 2, no. 1, pp. 11–20, 2020.

[24] M.Ş. Balcı and A. Dalcalı, "Design and Application of Optimum Toroidal Shaped Electromagnetic Energy Harvesters for Unmanned Aerial Vehicles", International Journal of Numerical Modelling: Electronic Networks, Devices and Fields, vol. 37, no. 3, 2024.

[25] T. Campi, S. Cruciani, F. Maradei and M. Feliziani, "Magnetic Field During Wireless Charging in an Electric Vehicle According to Standard SAE J2954", Energies, vol. 12, no. 9, 2019.

[26] G.A. Covic and J.T. Boys, "Inductive Power Transfer", Proceedings of the IEEE, vol. 101, no. 6, . 1276–1289, 2013.